c 2

NASA
Technical
Paper
1940

December 1981

Numerical Analysis of the Scramjet-Inlet Flow Field by Using Two-Dimensional Navier-Stokes Equations

Ajay Kumar

NASA

NASA Technical Paper 1940

1981

Numerical Analysis of the Scramjet-Inlet Flow Field by Using Two-Dimensional Navier-Stokes Equations

Ajay Kumar
Langley Research Center
Hampton, Virginia

NASA
National Aeronautics and Space Administration

Scientific and Technical Information Branch

SUMMARY

A computer code has been developed to solve the full Navier-Stokes equations in a supersonic combustion ramjet (scramjet) inlet. In order to be able to consider a general inlet geometry with embedded bodies, a numerical coordinate transformation is used which generates a set of boundary-fitted curvilinear coordinates. The physical domain is transformed into a rectangular computational domain with uniform mesh spacings. Embedded bodies are transformed into slits. MacCormack's unsplit, explicit, two-step, finite-difference method is used to solve the governing equations. An algebraic, two-layer eddy-viscosity model is used for the turbulent flow. The code can analyze both inviscid and viscous flows with no strut, one strut, or multiple struts in the flow field. A brief description is given of how this two-dimensional analysis can be used in a quasi three-dimensional form to analyze actual scramjet inlets. Detailed results are presented for one model inlet problem and several actual scramjet-inlet configurations. The application of the code in preliminary parametric design studies of a scramjet inlet is discussed briefly.

INTRODUCTION

The Langley Research Center is currently engaged in developing an airframe-integrated, hydrogen-fueled, supersonic combustion ramjet (scramjet) engine for hypersonic speeds. (See refs. 1 and 2.) Integration of the vehicle and propulsion system provides the use of the vehicle forebody to precompress the engine airflow before it enters the inlet and the use of the vehicle afterbody for additional expansion of the nozzle exhaust gas. Figure 1 shows the basic engine concept. It is seen that the entire under surface of the vehicle is part of the propulsion system. At a high Mach number, the need for integration arises because almost all of the airflow between the vehicle and its bow shock is required by the engine for good performance. This suggests an inlet capture area with an annular shape. By splitting the annular area into smaller rectangular modules, the primary engine becomes a system of identical units of size and shape appropriate for testing in ground facilities. One such rectangular module is shown in figure 2 with a cross-sectional view at the bottom of the figure. The module has a fixed-geometry inlet with wedge-shaped sidewalls. Sweep of these sidewalls, in combination with a recess in the cowl, allows spillage to occur efficiently with fixed geometry of the inlet. Inlet compression is completed by three wedge-shaped struts located at the minimum-area section.

Considerable aerodynamic testing over a period of years has resulted in an inlet design which performs well over a wide Mach number range. The basic design features of this inlet are described in reference 3. A problem, that has been shown to exist by the experimental work, is an interaction between the combustion-induced disturbances and the inlet flow; this has resulted in either increased spillage from the inlet or complete engine unstart. Although this interaction problem is being investigated in further inlet and engine tests, it has not yet been addressed analytically and will not be addressed herein. However, with the availability of high-speed computers and advanced computing techniques, it is now feasible to study the flow analytically in an isolated scramjet inlet. This will not only help in analyzing the problems observed experimentally but will also allow a parametric study in the future inlet designs with a substantial reduction in cost and time.

The flow in the scramjet inlet is highly three dimensional, possibly turbulent, and has complex shock—expansion-wave interactions. It also involves strong shock—boundary-layer interactions which may result in separated regions. To analyze such flows, it is necessary to use the full Navier-Stokes equations with proper turbulence modeling. Previous analytical work for the scramjet inlet has been very limited, confined only to inviscid two-dimensional flows using shock fitting techniques. (See refs. 3 and 4.) The objective of the present work is to develop a numerical computer code which can analyze the viscous flow in the scramjet inlet. A two-dimensional computer code has been developed initially to gain understanding of some features of the inlet flow.

The analysis as such uses the two-dimensional Navier-Stokes equations in conservative law form to describe the inlet flow. A two-layer eddy-viscosity model due to Baldwin and Lomax (ref. 5) is used for the turbulent flow. In order to facilitate the usage of a general inlet geometry with embedded bodies, a numerical coordinate transformation is used which generates a set of boundary-fitted curvilinear coordinates. (See refs. 6 and 7.) It transforms the physical domain into a rectangular domain with uniform mesh spacing, and embedded bodies in the flow field are transformed into slits. The transformation allows for concentrating mesh lines in regions of high gradients. The transformed governing equations are solved by an unsplit, explicit, two-step, finite-difference method due to MacCormack. (See ref. 8.) This explicit method is highly efficient on the vector-processing Control Data CYBER 203 computer for which the current computer code is written.

The code, in its present form, can analyze two-dimensional inviscid and viscous (laminar and turbulent) flows with no strut, one strut, or multiple struts in the flow field. In order to explore the potential of the code, several model inlet problems have been solved. The results for one such problem are presented herein. A brief description is given of how this two-dimensional analysis can be used in a quasi three-dimensional form to analyze actual scramjet inlets. Detailed results for inlets having one, two, and three struts are presented herein.

SYMBOLS

H	total enthalpy
h	static enthalpy
i,j	x and y grid indices, respectively
J	Jacobian determinant
M_1	Mach number at face of inlet
$M_{1,N}$	component of M_1 normal to sidewall leading-edge sweep
$M_{1,t}$	component of M_1 tangential to sidewall leading-edge sweep
M_∞	free-stream Mach number
$N_{Pr,\ell}$	laminar Prandtl number
$N_{Pr,t}$	turbulent Prandtl number

N_{Re} Reynolds number

n number of time-steps

p pressure

p_1 pressure at face of inlet

q_x, q_y components of heat flux in x,y-system

R gas constant

T temperature

T_1 temperature at face of inlet

t time

u,v components of velocity in x,y-system

$\bar{u}, \bar{v}$ transformed velocities defined in equation (3)

x,y Cartesian coordinates

Λ sweep angle of sidewall leading edge

μ effective viscosity, $\mu_\ell + \mu_t$

μ_ℓ laminar viscosity

μ_t turbulent viscosity

ζ, η transformed coordinates

ρ density

$\sigma_x, \sigma_y, \tau_{yx}$ components of stress tensor in x,y-system

ANALYSIS

Coordinate Transformation

In order to facilitate the usage of a general inlet geometry with embedded bodies, a numerical coordinate transformation is employed which generates a set of boundary-fitted curvilinear coordinates, $\zeta(x,y)$ and $\eta(x,y)$. It transforms the physical domain into a rectangular domain with uniform mesh spacings in the ζ- and η-directions. Embedded bodies in the flow field are transformed into slits. Figure 3 illustrates the coordinate transformation. Figure 3(a) shows a two-dimensional geometry in the physical plane, where a strut EFGH is seen sitting in the flow field. Figure 3(b) shows the geometry in the transformed plane. The outer boundary ABCD is transformed into a rectangle A'B'C'D', and the strut EFGH is transformed into a slit E'G'. The upper surface of the strut is made coincident with one of the mesh lines, and the lower surface of the strut is treated separately. The transformation allows for concentrating the mesh lines in regions of

high gradients such as around the strut or near boundary surfaces. A typical grid is shown in figure 3(c) downstream of line ZZ'. Every other grid point is plotted in the y-direction.

The coordinates in the present analysis are obtained by using the approach of Thompson et al. (ref. 6) in which $\zeta(x,y)$ and $\eta(x,y)$ are solutions of the equations

$$\left.\begin{aligned} \nabla^2\zeta &= P(\zeta,\eta) \\ \nabla^2\eta &= Q(\zeta,\eta) \end{aligned}\right\} \tag{1}$$

where ∇^2 is the Laplacian operator $(\partial^2/\partial x^2 + \partial^2/\partial y^2)$. Both $P(\zeta,\eta)$ and $Q(\zeta,\eta)$ are the source terms used to control the spacing of ζ = Constant and η = Constant lines in the physical plane. In the present analysis, these terms are in the form described in reference 6. The coordinates $\zeta(x,y)$ and $\eta(x,y)$ are subject to Dirichlet boundary conditions along boundaries AC and BD and Neumann boundary conditions along boundaries AB and CD. The Navier-Stokes equations are solved in the transformed plane, and the inlet flow field in the physical plane is obtained by using the inverse transformation $x(\zeta,\eta)$ and $y(\zeta,\eta)$.

The aforementioned transformation has indirect grid control and requires an iterative procedure to solve the set of two-dimensional elliptic equations which make it complex and time consuming. Its extension to three-dimensional domains becomes even more complex and time consuming. In future application of the code developed herein, an algebraic numerical transformation (ref. 7) will be used which allows for direct grid control. This transformation is suitable for three dimensions and is very inexpensive since it uses algebraic relations to relate the physical domain to the computational domain.

Governing Equations

Two-dimensional Navier-Stokes equations in fully conservative form are used to describe the inlet flow. The transformed equations can be written as

$$\frac{\partial U}{\partial t} + \frac{\partial M}{\partial \zeta} + \frac{\partial N}{\partial \eta} = 0 \tag{2}$$

where

$$U = J\begin{bmatrix} \rho \\ \rho u \\ \rho v \\ \rho H - p \end{bmatrix}$$

$$M = \begin{bmatrix} \rho\bar{u} \\ \rho u\bar{u} + y_\eta \sigma_x - x_\eta \tau_{yx} \\ \rho v\bar{u} + y_\eta \tau_{xy} - x_\eta \sigma_y \\ \rho H\bar{u} - p\bar{u} + y_\eta(u\sigma_x + q_x) - x_\eta(v\sigma_y + q_y) + \tau_{yx}(vy_\eta - ux_\eta) \end{bmatrix}$$

$$N = \begin{bmatrix} \rho\bar{v} \\ \rho u\bar{v} - y_\zeta \sigma_x + x_\zeta \tau_{yx} \\ \rho v\bar{v} - y_\zeta \tau_{yx} + x_\zeta \sigma_y \\ \rho H\bar{v} - \rho\bar{v} - y_\zeta(u\sigma_x + q_x) + x_\zeta(v\sigma_y + q_y) + \tau_{yx}(-vy_\zeta + ux_\zeta) \end{bmatrix}$$

Here, x_ζ denotes $\partial x/\partial\zeta$, and so forth, and

$$\left.\begin{aligned} \bar{u} &= y_\eta u - x_\eta v \\ \bar{v} &= -y_\zeta u + x_\zeta v \\ J &= x_\zeta y_\eta - x_\eta y_\zeta \end{aligned}\right\} \tag{3}$$

The quantities σ_x, σ_y, and τ_{yx} are components of the stress tensor and are given by

$$\left.\begin{aligned} \sigma_x &= p + \frac{2\mu}{3}\frac{\partial v}{\partial y} - \frac{4\mu}{3}\frac{\partial u}{\partial x} \\ \sigma_y &= p + \frac{2\mu}{3}\frac{\partial u}{\partial x} - \frac{4\mu}{3}\frac{\partial v}{\partial y} \\ \tau_{yx} &= -\mu\left(\frac{\partial u}{\partial y} + \frac{\partial v}{\partial x}\right) \end{aligned}\right\} \tag{4}$$

The quantities q_x and q_y are components of the heat flux and are given by

$$q_x = -\left(\frac{\mu_\ell}{N_{Pr,\ell}} + \frac{\mu_t}{N_{Pr,t}}\right)\frac{\partial h}{\partial x} \tag{5a}$$

$$q_y = -\left(\frac{\mu_\ell}{N_{Pr,\ell}} + \frac{\mu_t}{N_{Pr,t}}\right)\frac{\partial h}{\partial y} \tag{5b}$$

In order to complete the set of governing equations, equation of state $p = \rho RT$ is used, where R is the gas constant.

In equations (4), μ is the sum of laminar viscosity and turbulent viscosity. The laminar viscosity for air is calculated from Sutherland's formula. The turbulent viscosity is calculated from an algebraic, two-layer eddy-viscosity model developed by Baldwin and Lomax. (See ref. 5.) Use of this model does not require the knowledge of the boundary-layer thickness; instead, the model uses the vorticity at each point in the flow field to characterize the scale of turbulence. The model as such consists of an inner law and an outer law. The inner law is applicable from the wall out to the location in the flow where the eddy viscosity given by the inner law is equal to that of the outer law. The outer law then is assumed applicable for the remainder of the flow. Details of the model are given in reference 5 along with the values of various constants used in the model.

Method of Solution

The governing equations are solved by an unsplit, explicit, two-step, finite-difference method developed by MacCormack. (See ref. 8.) This explicit method has second-order accuracy in both space and time and is highly efficient on the Control Data CYBER 203 vector-processing computer for which the current code is written. If a solution to equation (2) is known at some time $t = n\,\Delta t$, the solution at the next time-step, $t = (n + 1)\,\Delta t$ can be obtained from

$$U_{i,j}^{n+1} = L(\Delta t)\, U_{i,j}^{n} \tag{6}$$

for each node point (i,j). The finite-difference operator L consists of a predictor step and a corrector step. Spatial derivatives in the predictor step are calculated by forward differences, whereas in the corrector step they are calculated by backward differences. The shear stress and heat-flux terms appearing in equations for M and N are backward differenced in the predictor step and forward differenced in the corrector step. When this method was applied to a two-dimensional, symmetric converging duct, it was found that the symmetry of the flow field is better achieved by reversing the order of differencing for the predictor and corrector steps from one time-step to the next time-step; that is, if forward and backward differences are used in time-step n, then backward and forward differences should be used in time-step $n+1$. The order of differencing is also reversed for shear and heat-flux terms. Details of the method and expressions for the predictor and corrector steps are given in reference 8.

A fourth-order numerical damping, given in reference 9, is used in the present analysis to damp the oscillations which occur in the neighborhood of strong shocks in the flow field.

Boundary and Initial Conditions

The flow variables at the inflow boundary are held fixed at given free-stream values, whereas first-order extrapolation is used to obtain the flow variables at the outflow boundary. For viscous flows, no-slip and adiabatic-wall conditions are applied. Along the lower wall, for example,

$$u_{i,j=1} = 0$$

$$v_{i,j=1} = 0$$

$$T_{i,j=1} = T_{i,j=2}$$

The pressure is determined from the boundary condition that the normal derivative of p vanishes, which is approximated by $\partial p/\partial \eta = 0$, resulting in

$$p_{i,j=1} = p_{i,j=2}$$

For inviscid flows, the tangency condition is satisfied on the surfaces; that is, $\bar{v} = 0$. The pressure and temperature are extrapolated from the interior grid points, and $\bar{u}$ is obtained from the total enthalpy which is held constant.

The aforementioned boundary conditions are applied in both the predictor and corrector steps. Initial conditions are normally prescribed for each set of calculations by assuming that free-stream conditions exist at all the grid points except at the boundaries where proper boundary conditions are applied.

Computational Grid and Time Requirements

All the computations are made on the Control Data CYBER 203 vector-processing computer (an upgraded version of the Control Data STAR 100 computer) by using the 64-bit arithmetic. A grid of 51 × 51 is used in the calculations which requires approximately 200 K computer storage. The solution advances about 20 time-steps per sec for the viscous flow and about 30 time-steps per sec for the inviscid flow. When the change in the density over two time-steps is of the order of 10^{-4}, the solution is assumed converged. A typical solution is obtained in 2 to 5 min, depending upon the number of time-steps required for convergence.

DISCUSSION OF RESULTS

This section briefly describes how the two-dimensional analysis can be used for three-dimensional scramjet inlets under certain assumptions. Detailed results are presented for one model inlet problem and for several scramjet-inlet configurations. All the results presented herein are for air under the perfect gas assumption.

Model Inlet Problem

The geometry of the model inlet problem is shown in figure 4. The inlet length is 10 cm with an initial height of 1.5 cm. The calculations are made in the region starting 1 cm ahead of the inlet, thus bringing the total length to 11 cm. The top surface produces a 10° compression at $x = 1$ cm and then a 20° expansion at $x = 6$ cm. The cowl plate is located in such a way that the shock from the top surface does not hit it, thus allowing a fraction of the flow to spill out of the inlet. The dimensions in the model problem have been fixed on the basis of certain features of the engine inlet flow, such as spillage, but are not typical of the actual engine dimensions. As will be seen, the problem clearly brings out the importance of the viscous effects which are normally neglected or accounted for approximately. Calculations are made for the inviscid, laminar, and turbulent flow by using the following conditions at the inflow boundary of the inlet: $M_1 = 5.0$, $p_1 = 101\ 325$ Pa, and $T_1 = 293$ K.

Figures 5 and 6 show the velocity-vector field and pressure contours, respectively, downstream of line ZZ'. For clarity, these plots are shown in the region downstream of the expansion corner from $x = 6$ cm to the end of the inlet. Upstream of the expansion corner, the shock from the top surface turns the flow downward by about 10°. Because of this, some flow spills out of the inlet ahead of the cowl plate. The velocity-vector fields in figure 5 are plotted for the laminar and turbulent flows only. Every other grid point is plotted in the y-direction. It is seen that the laminar boundary layer on the top surface separates because of the interaction of the cowl shock with the boundary layer on the top surface. The separation completely disappears for the turbulent flow under the aforementioned flow conditions, since the turbulent boundary layer is able to accept higher adverse flow gradients without separating.

The pressure contours in figure 6 are shown for inviscid, laminar, and turbulent flows. These contour plots clearly show the interaction of the cowl shock with the expansion waves from the top surface. Due to this interaction, the shock hits the top surface earlier than it would have without the interaction. The expansion waves go through the shock and attenuate the pressure on the cowl plate, whereas the shock is reflected from the top surface. It is also seen that the point, at which the cowl shock hits the top surface, moves upstream with increasing viscous effects. Thus, it is necessary to include viscous effects in the inlet analysis to locate the waves in the flow field properly.

Figure 7 shows the pressure distribution on the top surface of the inlet for the inviscid flow. The pressure is seen to increase because of the compression at $x = 1$ cm. It remains constant until it is decreased because of the expansion at $x = 6$ cm. It again remains constant until the cowl-plate shock hits the top surface which increases the pressure. The gradual decrease in the surface pressure toward the end of the inlet is due to the expansion waves which hit the top surface after being reflected from the cowl plate. The pressure distribution from the exact shock—expansion-wave theory is also shown in figure 7 for comparison with the present calculations. The exact results are shown only up to the point where the cowl shock hits the top surface. It is seen that the present results are in excellent agreement with the exact calculations.

As mentioned earlier, the geometry of the problem is such that some flow spills out of the lower boundary. The spillage, as calculated by the present analysis, is 29.8 percent for the inviscid flow, 36.3 percent for the laminar flow, and 43.2 percent for the turbulent flow. The exact values for the inviscid flow are 31.4 percent

for 10° compression, 36.7 percent for 10.5° compression, and 42.3 percent for 11° compression. This implies that the effective change in the body compression angle due to viscous effects is approximately 0.5° for the laminar flow and 1° for the turbulent flow, which compares well with the estimates based on the boundary-layer displacement-thickness calculations.

The results of the model problem show that the present code predicts the complex supersonic flow very well. In the following section, the code is used to analyze actual scramjet-inlet configurations under certain assumptions.

Quasi Three-Dimensional Technique

In this section a brief description is given to explain how the two-dimensional analysis may be used in a quasi three-dimensional sense to analyze scramjet inlets. The technique is verified by calculating the flow field for a three-strut inlet for which experimental results are available.

The following sketch shows the side view of a scramjet module:

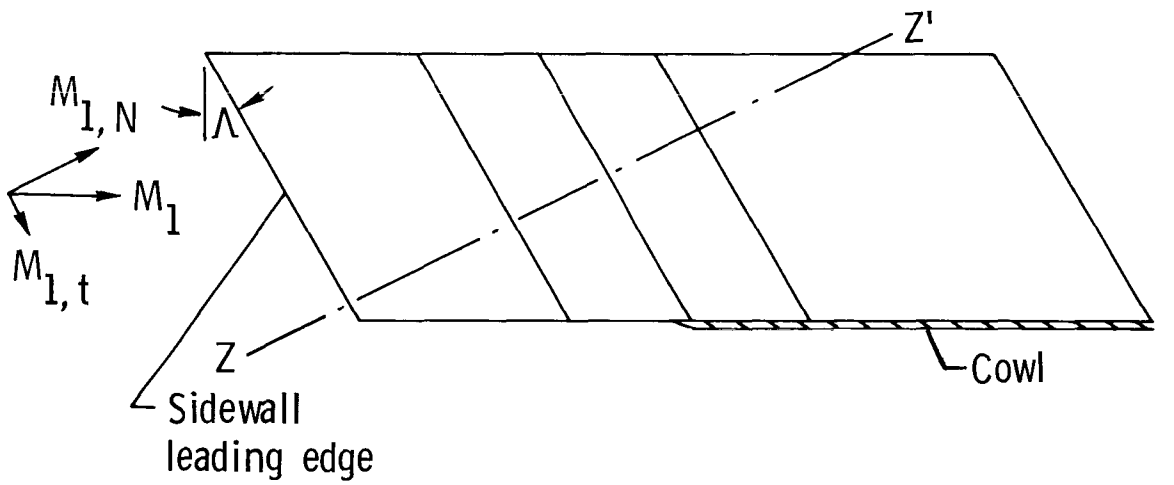

All the compression surfaces are swept back at an angle Λ, and the Mach number at the face of the inlet is M_1. If the shock waves in the inlet do not detach and if the end effects are neglected, the component of the velocity parallel to sidewall sweep should remain unchanged, and the flow disturbances should occur in the plane ZZ' normal to the sidewall leading edge. The flow can, therefore, be solved by using the two-dimensional code in the plane ZZ' with Mach number $M_{1,N}$. The solution in the ZZ' plane can be projected to the plane of the cowl, and the velocity distribution in the plane of the cowl can be obtained by superimposing the constant velocity component over the aforementioned solution. In case of viscous flows, an approximate boundary-layer profile has to be prescribed for the constant tangential velocity component before superimposing it. By knowing the velocity and density distributions it is possible to estimate the flow spillage from this class of three-dimensional inlets as a function of cowl location. Thus, the two-dimensional analysis may be used in preliminary parametric design studies of the scramjet inlet to determine the effects of various parameters such as sweep of the sidewalls, number of struts and their locations and shapes, cowl location and its shape, and others. As will be seen, the analysis can also give an indication as to whether the inlet will operate for a given set of flight conditions.

By using this approach the two-dimensional code is used to analyze the three-strut scramjet-inlet configuration, details of which are given in reference 3. The inlet sidewalls are swept at an angle of 48°. Figure 8 shows a comparison of the turbulent sidewall pressure distribution. The experimental measurements have been made in a plane parallel to the cowl which is located at about half of the inlet height. This particular plane is chosen for comparison purposes so that the cowl shock does not affect the measured sidewall pressures up to the point of comparison in the axial direction. (The present analysis cannot account for the cowl shock disturbances.) It is seen from figure 8 that the present calculations are in very good agreement with the measured values. The present analysis estimates an inlet capture of about 97 percent which is slightly higher than the experimentally measured value of 94 percent. This is expected because the end effects, which are not accounted for in the present analysis, increase the flow spillage.

Parametric Study

Preceding results show the direct application of the two-dimensional code in analyzing the actual inlet configurations. The type of agreement obtained for the three-strut inlet gives credibility to the code in its use as a tool for parametric studies in inlet design. In the present study, this is done by analyzing one- and two-strut inlets over a range of Mach numbers. The sidewall leading-edge sweep for these inlets is prescribed as 33°. Realistic flow conditions are used in the analysis and are shown in the following table:

M_∞	M_1	$M_{1,N}$	p_1, MPa	T_1, K	N_{Re} per m
4	3.43	2.88	0.00963	322	5.43×10^6
5	4.29	3.60	.00648	328	4.57
6	5.18	4.34	.00456	329	3.88
7	6.00	5.032	.00355	335	3.49

Figure 9 shows the geometry of a one-strut inlet in a plane normal to the sidewall leading-edge sweep. The initial width of the inlet is 15 cm and other dimensions and angles are shown in the figure. Figure 10 shows the pressure contours for the inviscid flow at three Mach numbers. No solution could be obtained at the lowest Mach number, $M_{1,N} = 2.88$ ($M_\infty = 4$), for which the shock waves detached in the inlet. For this case, after a sufficient number of time-steps, a normal shock formed just downstream of the inflow boundary resulting in a large mass imbalance. The mass imbalance occurs when the governing equations fail to produce a solution for the prescribed inflow boundary conditions; that is, the inlet minimum-area section cannot pass the inflow mass and the flow chokes. It is seen from the contour plots in figure 10 that the shock wave from the sidewall coalesces with the shock wave from the strut leading edge to form a stronger shock. For the laminar flow, the strong shock, formed by the shock-wave coalescence, caused a large separated region on the sidewall which produced an induced shock in front of the separated region. The induced shock choked the flow in a manner similar to that described earlier, and again no meaningful solution could be obtained at any of the Mach numbers considered here. For the turbulent flow, the solution could be obtained at the highest Mach number, but the

flow choked again at lower Mach numbers. The following table summarizes the conditions for which the solutions could or could not be obtained (indicated by "yes" and "no," respectively):

Mach number, M_∞	Type of flow		
	Inviscid	Laminar	Turbulent
7	Yes	No	Yes
6	Yes	No	No
5	Yes	No	No
4	No	No	No

Figure 11 shows the variation of inviscid-flow spillage as a function of cowl location for $M_\infty = 7.0$. Spillage is calculated by assuming that the inlet height is equal to its initial width. The results obtained from the code of reference 4, which is a second-order numerical solution of the supersonic inviscid flow, are also shown in this figure. It is seen that the present calculations agree very well with those obtained from the code of reference 4.

In order to eliminate the problem of shock-wave coalescence in the one-strut inlet, a two-strut inlet is considered. The geometry of this inlet is shown in figure 12. The initial width of the inlet is again 15 cm. Other dimensions and angles are shown in the figure. The strut surface, on which the shock from the sidewall strikes, is kept parallel to the oncoming flow so that no shock is produced by this surface. This avoids the possibility of shock-wave coalescence. Figure 13 shows the pressure contours for the laminar flow at three Mach numbers. The corresponding velocity-vector fields are shown in figure 14. No viscous-flow solution could be obtained for the lowest Mach number because of the choking of the flow caused by the boundary-layer separation. The solutions could be obtained at all Mach numbers for the inviscid flow. The following table summarizes the conditions for which the solutions could or could not be obtained (indicated again by "yes" and "no," respectively):

Mach number, M_∞	Type of flow		
	Inviscid	Laminar	Turbulent
7	Yes	Yes	Yes
6	Yes	Yes	Yes
5	Yes	Yes	Yes
4	Yes	No	No

The table clearly shows the improvement in the performance of the two-strut inlet over the one-strut inlet.

The preceding parametric study indicates that the numerical computer code developed herein can be used to modify or eliminate some of the designs or flow conditions which are not expected to perform well and, thus, can help in reducing the experimental testing required for inlet design.

CONCLUDING REMARKS

Two-dimensional Navier-Stokes equations have been used to analyze the flow in a supersonic combustion ramjet (scramjet) inlet. The analysis uses a numerical coordinate transformation which generates a set of boundary-fitted curvilinear coordinates. The embedded bodies in the flow field are transformed into slits. MacCormack's unsplit, explicit, two-step, finite-difference method is used to solve the governing equations. A two-layer eddy-viscosity model is used for the turbulent flow. The numerical computer code can analyze both inviscid and viscous flows with no strut, one strut, or multiple struts in the flow field.

Results are presented for one model inlet problem and for several actual scramjet-inlet configurations. In all these cases, the code predicted the complex wave interactions and shock—boundary-layer interactions very well. The application of the two-dimensional analysis in the preliminary parametric design studies of a scramjet inlet is discussed briefly. It is shown that the two-dimensional analysis can give an indication as to whether the inlet will operate for a given set of flight conditions.

Langley Research Center
National Aeronautics and Space Administration
Hampton, VA 23665
October 6, 1981

REFERENCES

1. Jones, Robert A.; and Huber, Paul W.: Toward Scramjet Aircraft. Astronaut. & Aeronaut., vol. 16, no. 2, Feb. 1978, pp. 38-48.

2. Beach, H. Lee, Jr.: XII. Hypersonic Propulsion. Aeropropulsion 1979, NASA CP-2092, 1979, pp. 387-400.

3. Trexler, Carl A.; and Souders, Sue W.: Design and Performance at a Local Mach Number of 6 of an Inlet for an Integrated Scramjet Concept. NASA TN D-7944, 1975.

4. Salas, Manuel D.: Shock Fitting Method for Complicated Two-Dimensional Supersonic Flows. AIAA J., vol. 14, no. 5, May 1976, pp. 583-588.

5. Baldwin, Barrett; and Lomax, Harvard: Thin-Layer Approximation and Algebraic Model for Separated Turbulent Flows. AIAA Paper 78-257, Jan. 1978.

6. Thompson, Joe F.; Thames, Frank C.; and Mastin, C. Wayne: Boundary-Fitted Curvilinear Coordinate Systems for Solution of Partial Differential Equations on Fields Containing Any Number of Arbitrary Two-Dimensional Bodies. NASA CR-2729, 1977.

7. Smith, Robert E.; and Weigel, Barbara L.: Analytic and Approximate Boundary-Fitted Coordinate Systems for Fluid Flow Simulation. AIAA-80-0192, Jan. 1980.

8. MacCormack, Robert W.: The Effect of Viscosity in Hypervelocity Impact Cratering. AIAA Paper No. 69-354, Apr.-May 1969.

9. Drummond, J. Philip: Numerical Investigation of the Perpendicular Injector Flow Field in a Hydrogen Fueled Scramjet. AIAA Paper 79-1482, July 1979.

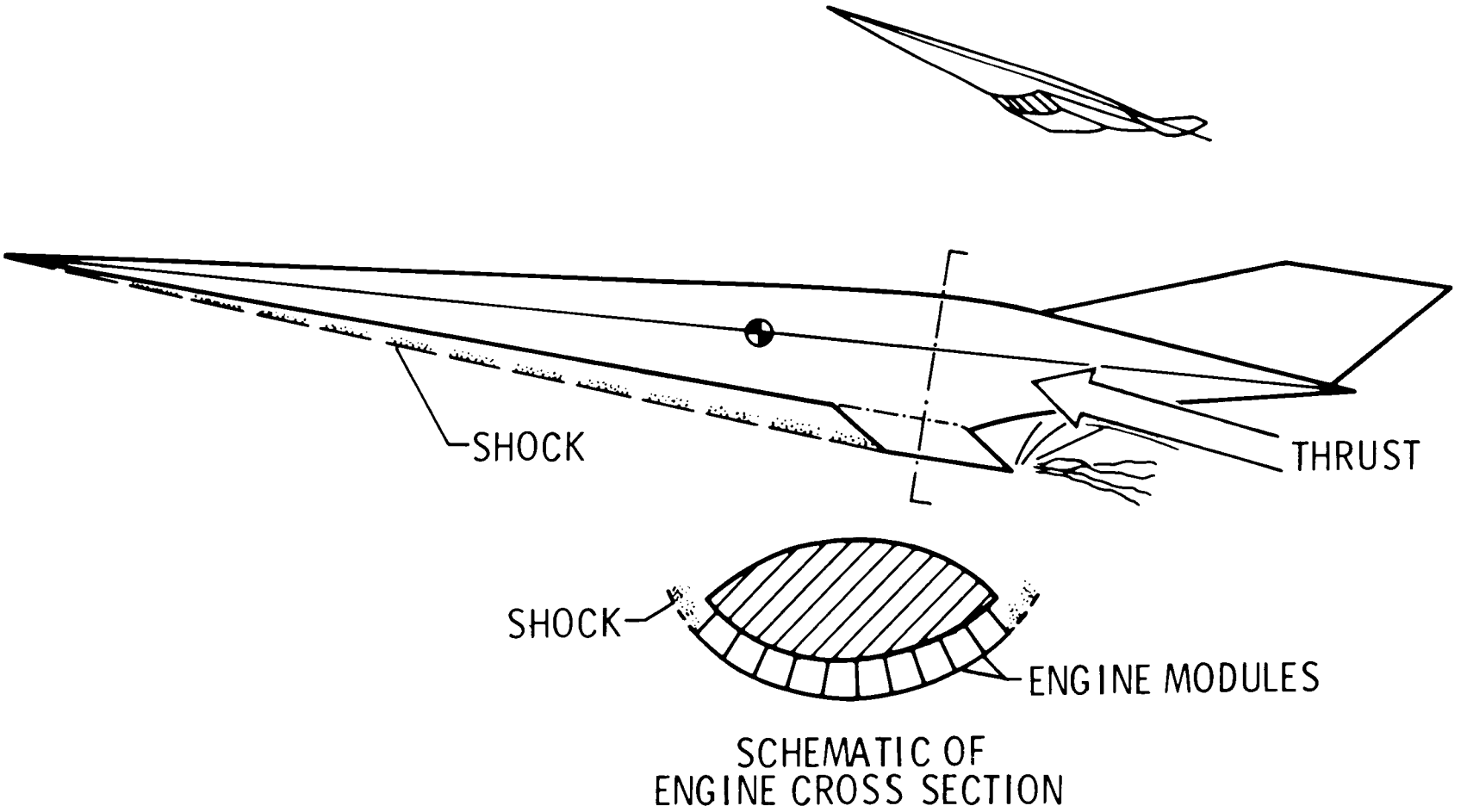

Figure 1.- Airframe-integrated scramjet-engine concept.

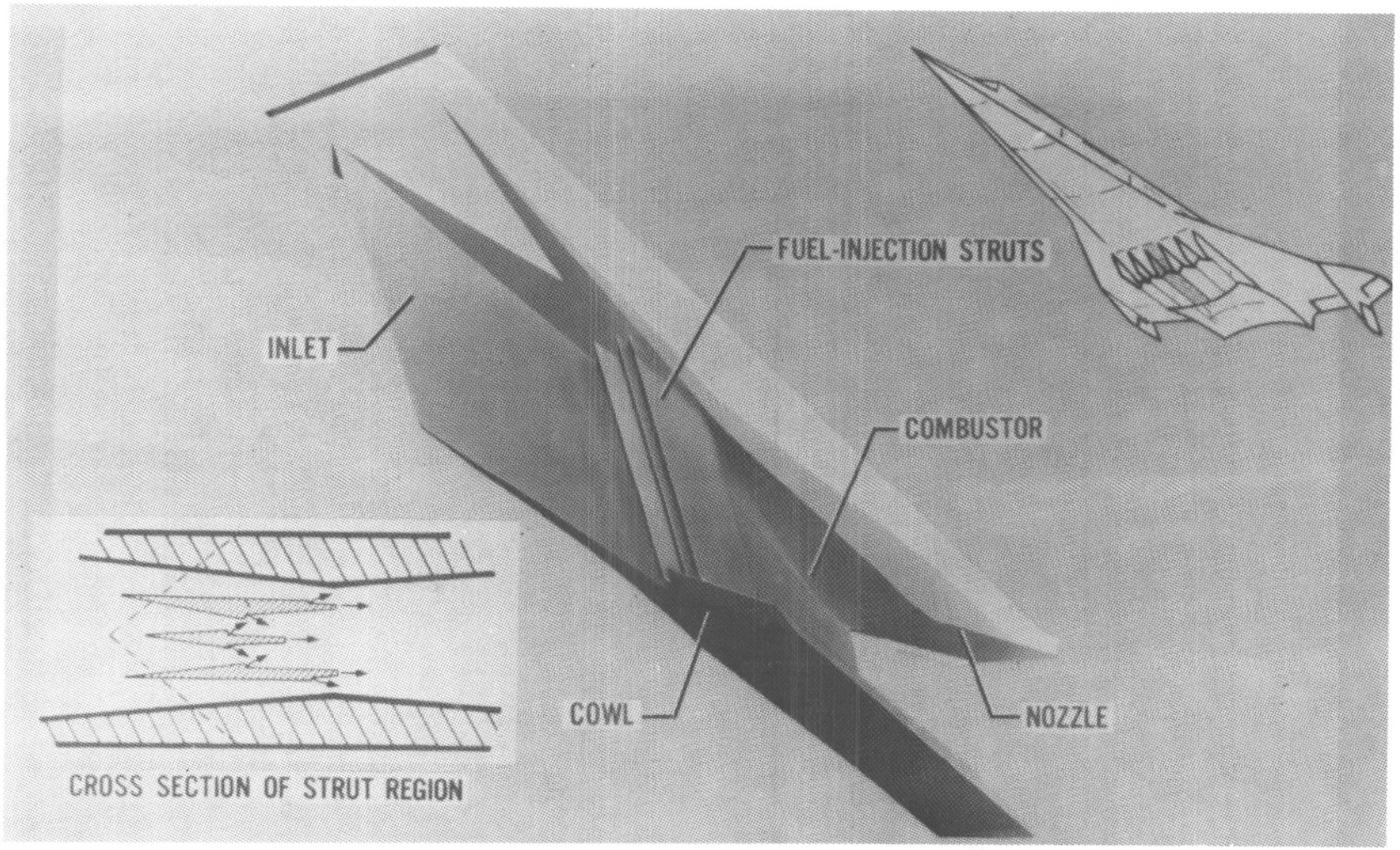

L-81-237

Figure 2.- Scramjet-engine module and its cross section.

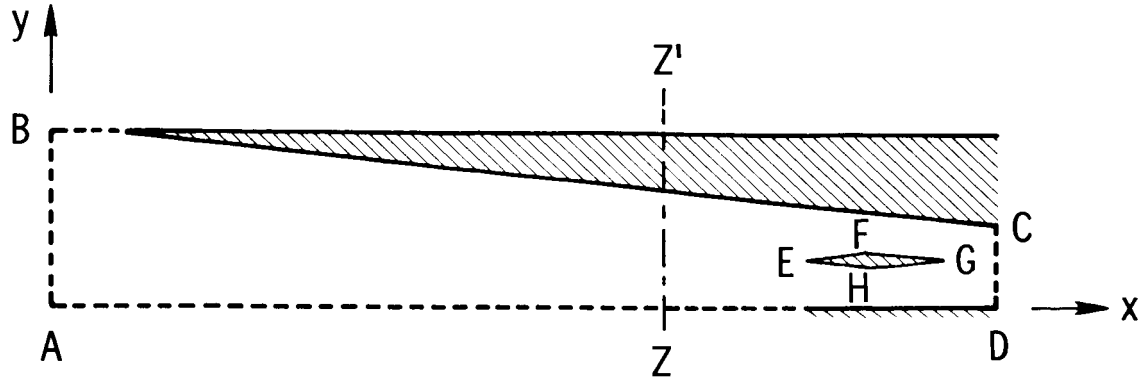

(a) Physical plane.

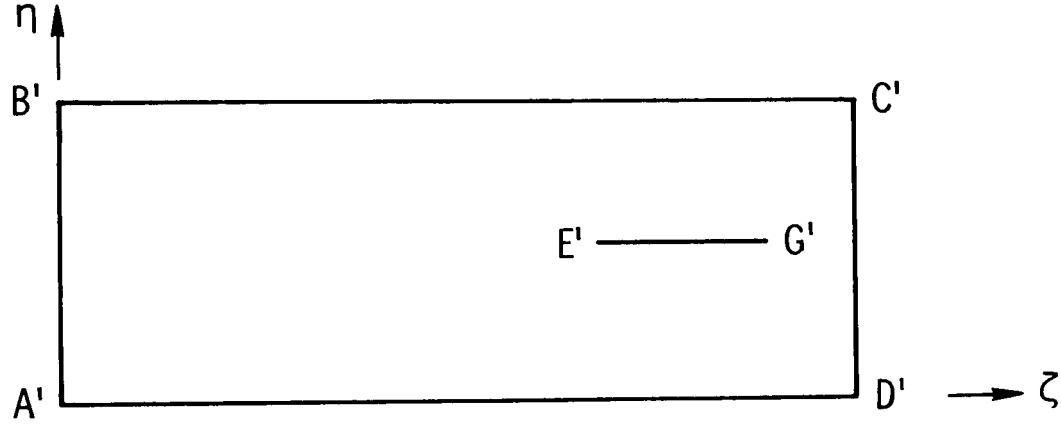

(b) Transformed plane.

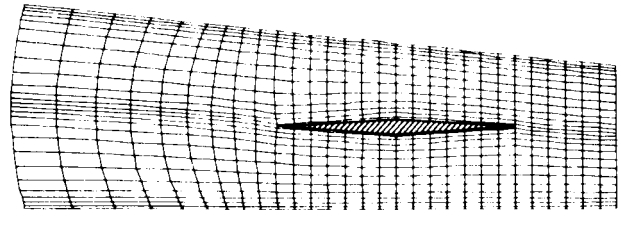

(c) Grid downstream of line ZZ'.

Figure 3.- An example of numerical coordinate transformation.

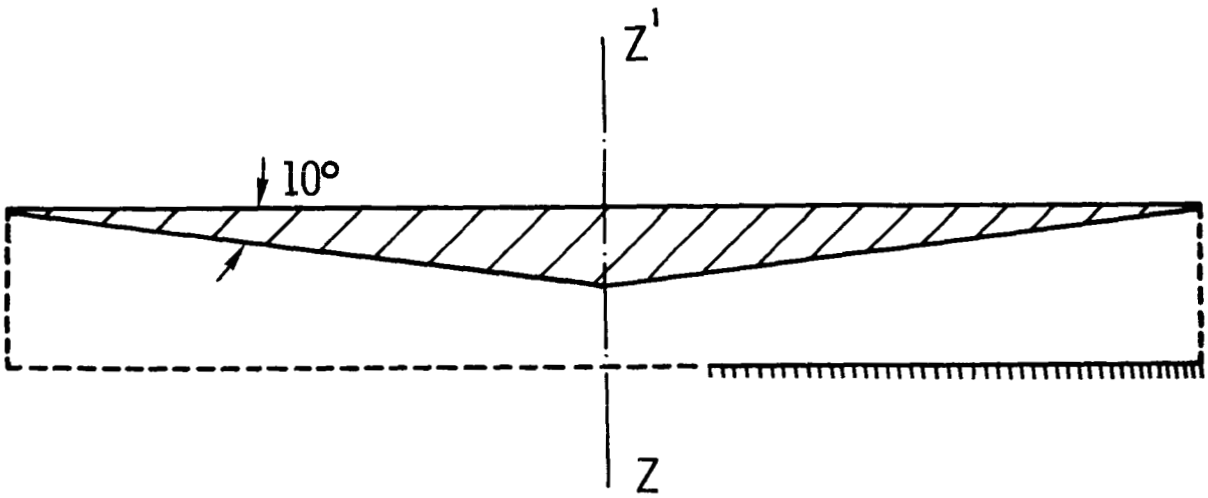

Figure 4.- Geometry of the model inlet problem.

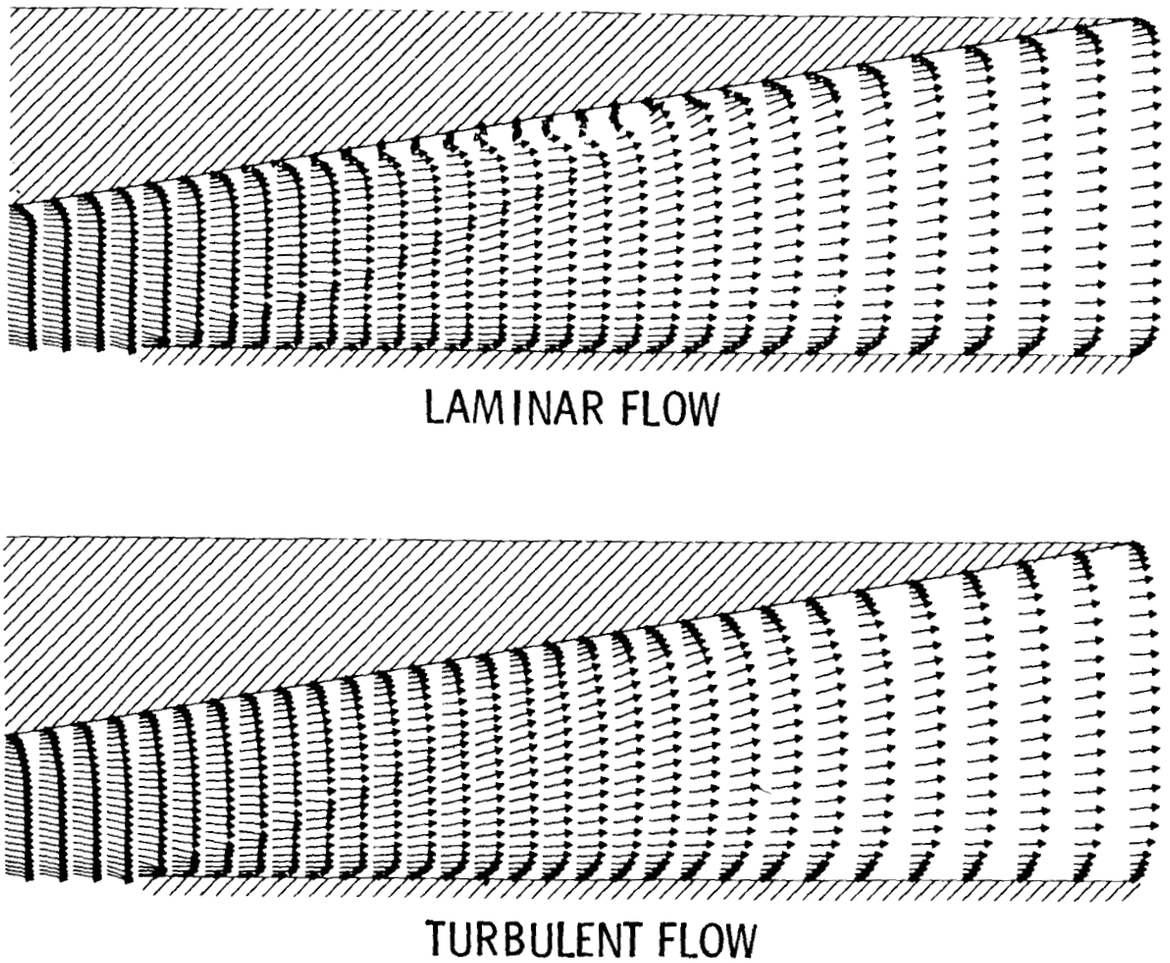

Figure 5.- Velocity-vector field downstream of line ZZ'.

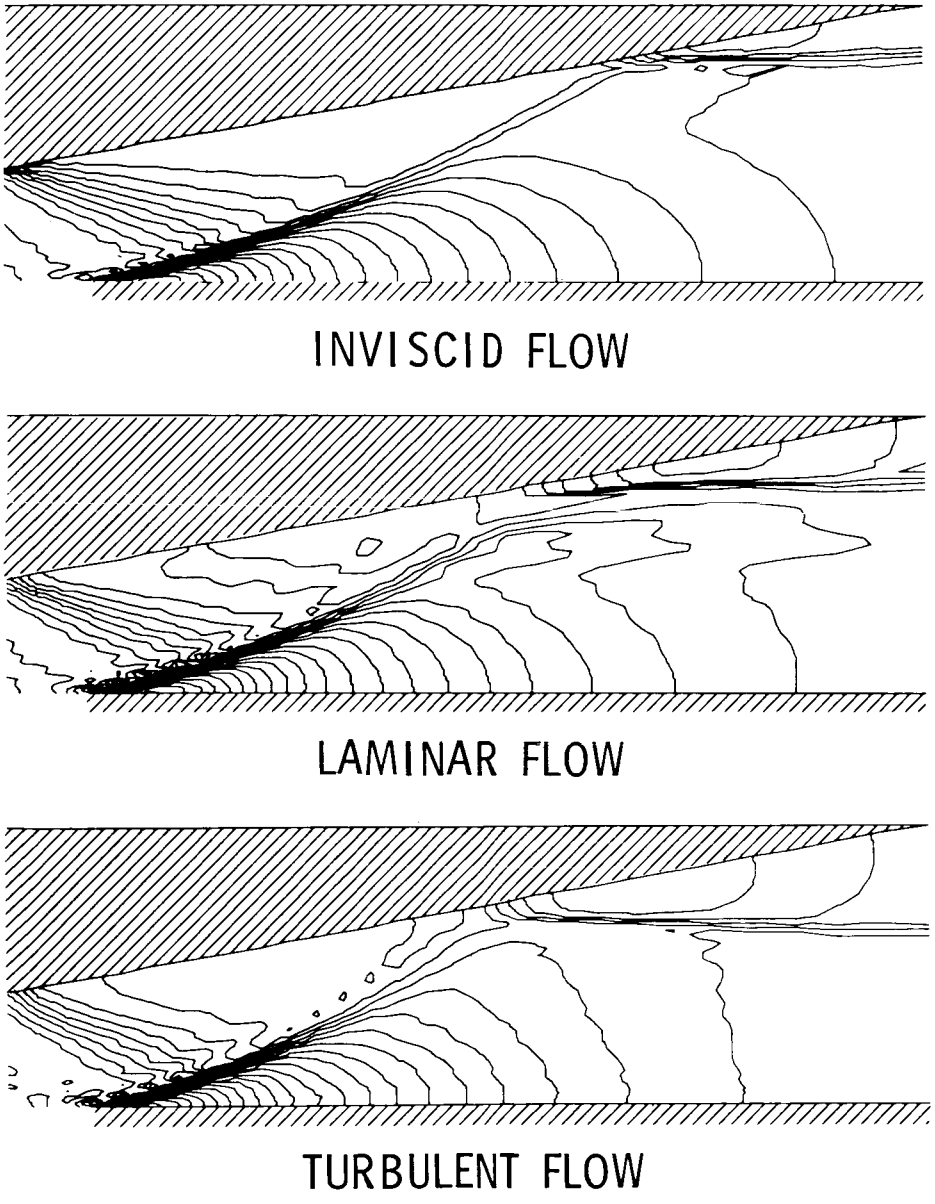

Figure 6.- Pressure contours downstream of line ZZ'.

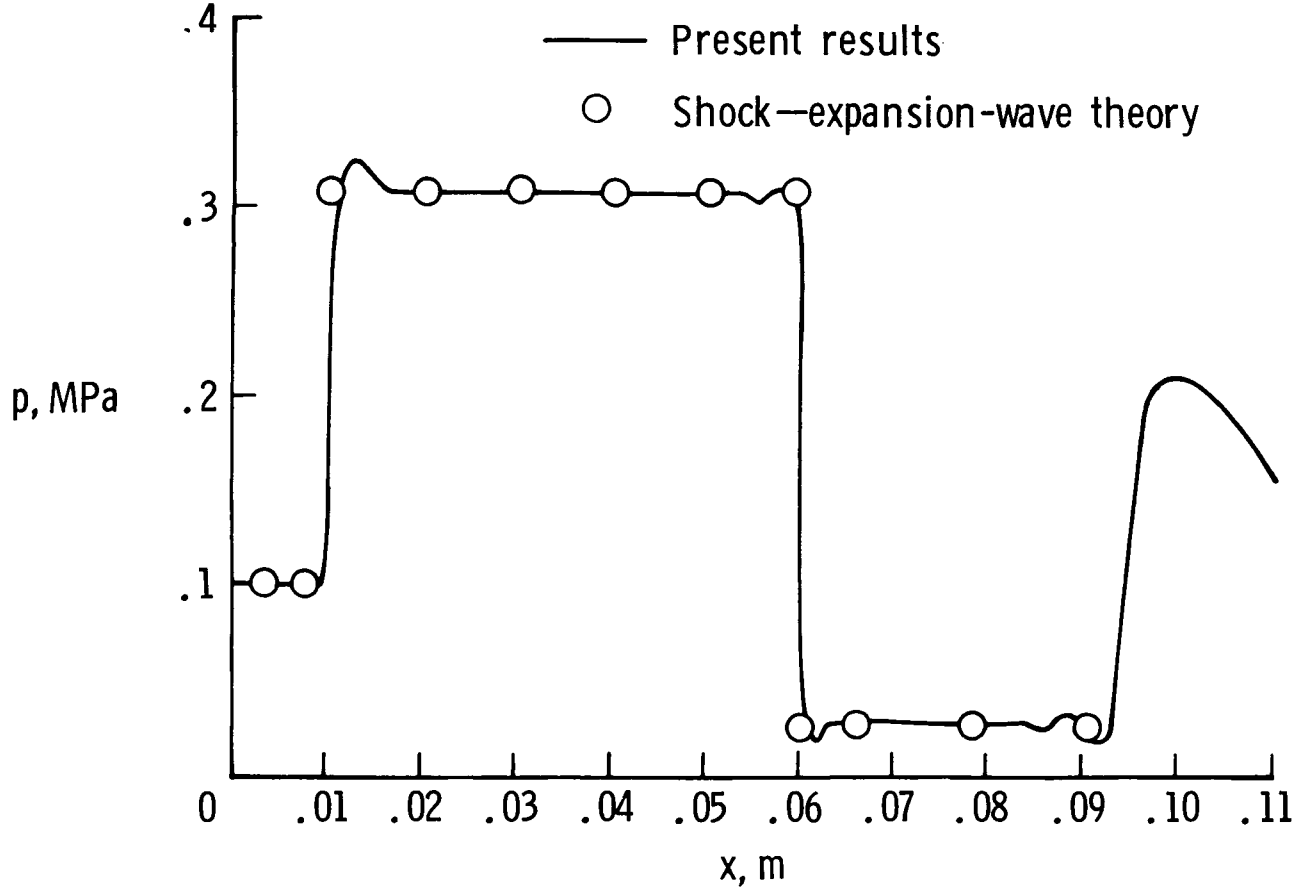

Figure 7.- Pressure distribution on the top surface of the inlet for inviscid flow.

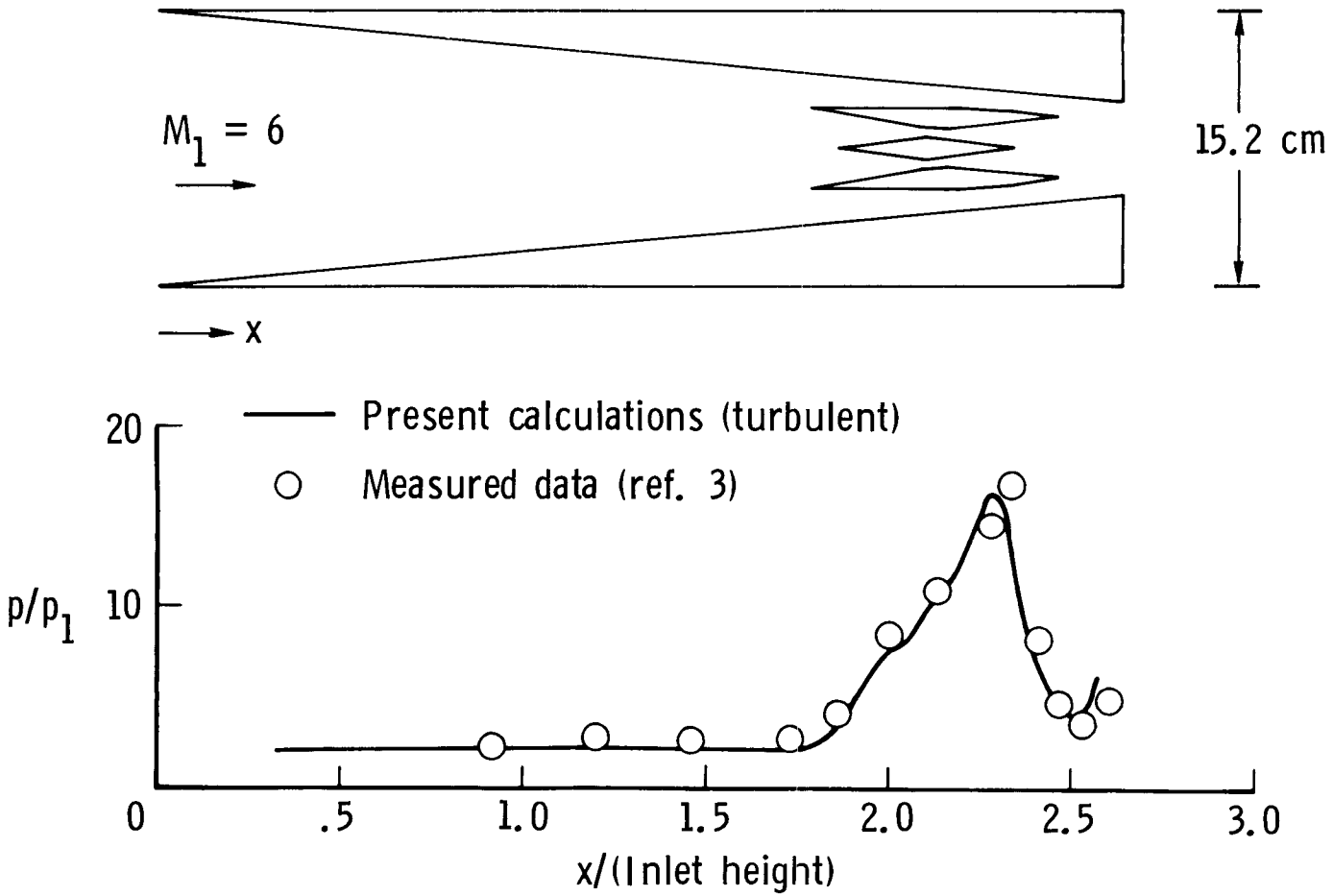

Figure 8.- Comparison of turbulent sidewall pressure distribution for a three-strut inlet. T_1 = 57 K; p_1 = 764 Pa; inlet height, 19 cm.

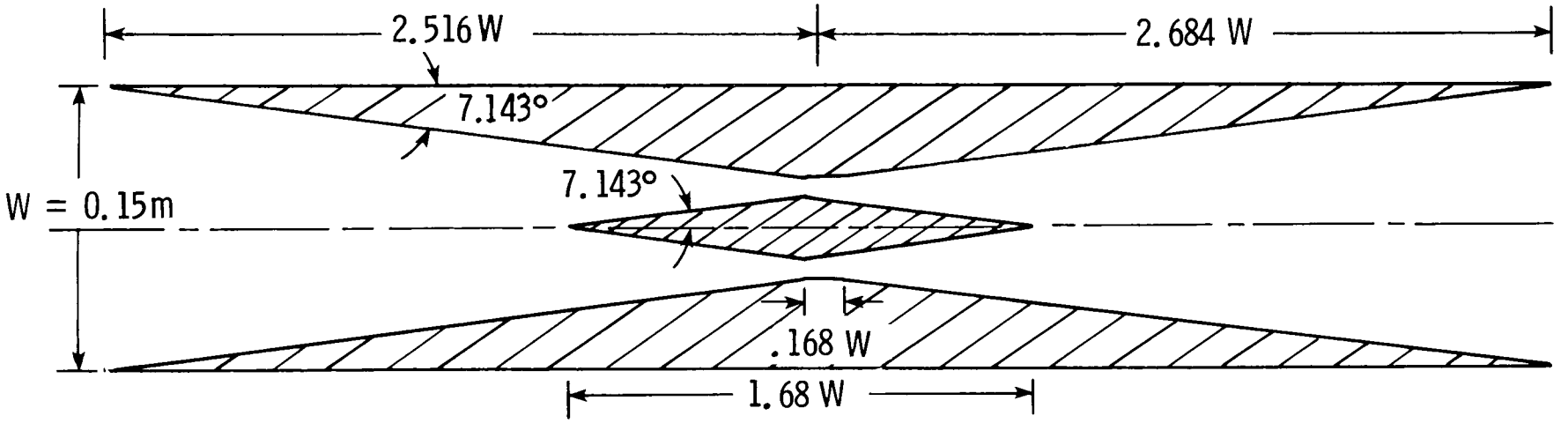

Figure 9.- Geometry of a one-strut inlet in a plane normal to sidewall leading-edge sweep.

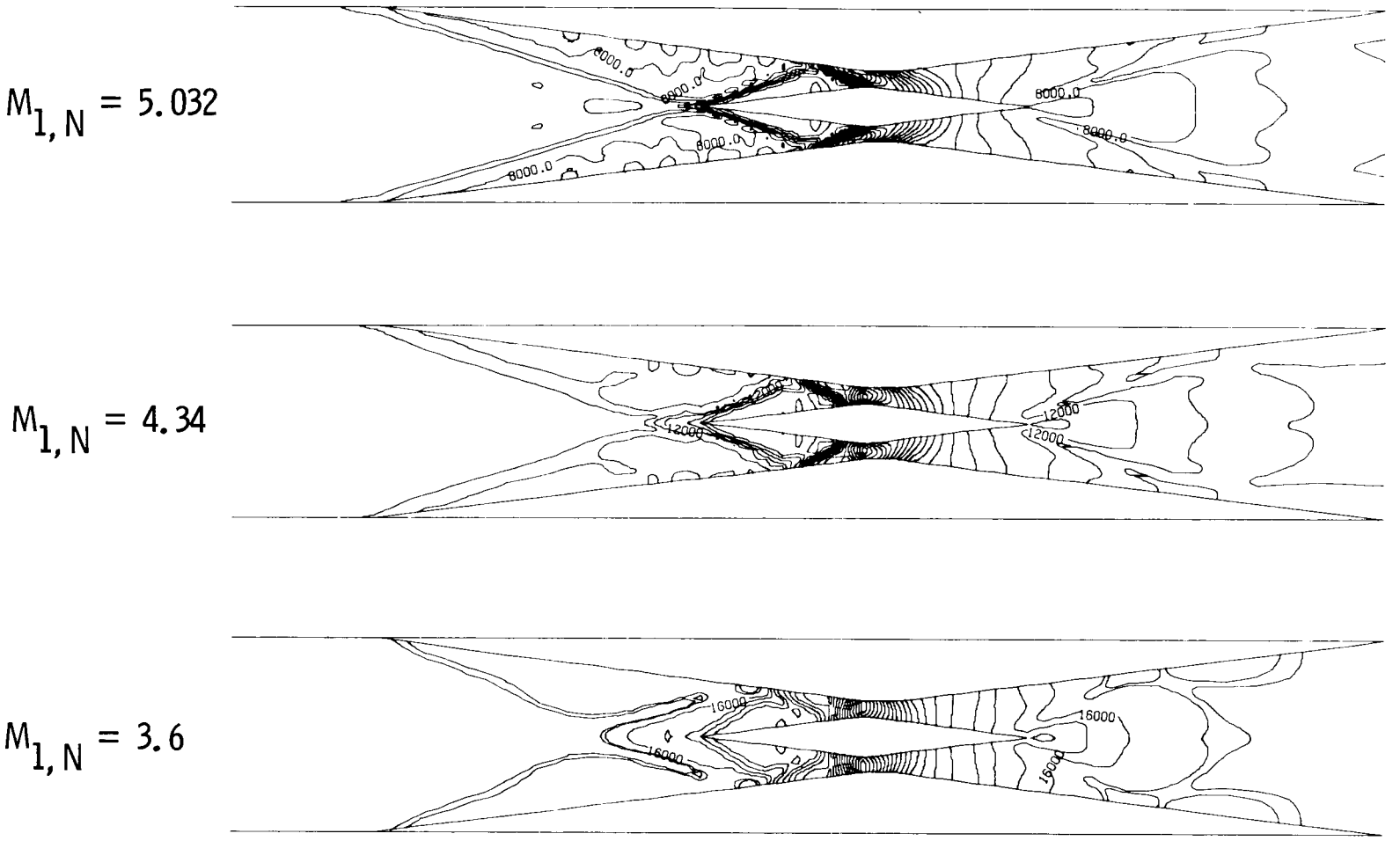

Figure 10.- Pressure contours for inviscid flow at three Mach numbers.

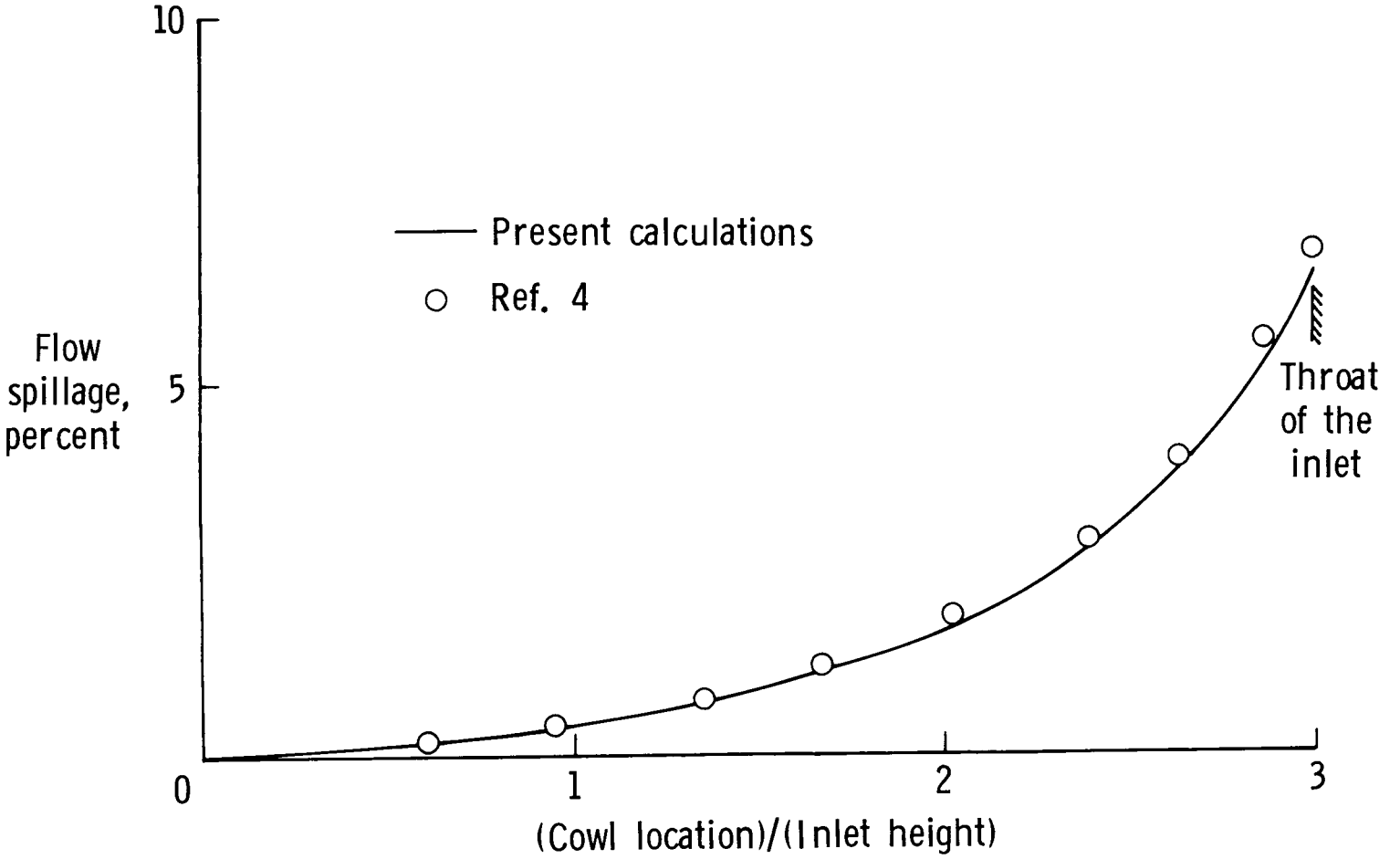

Figure 11.- Comparison of inviscid-flow spillage for a one-strut inlet. Inlet height, 15 cm; $\Lambda = 33°$; $M_\infty = 7.0$.

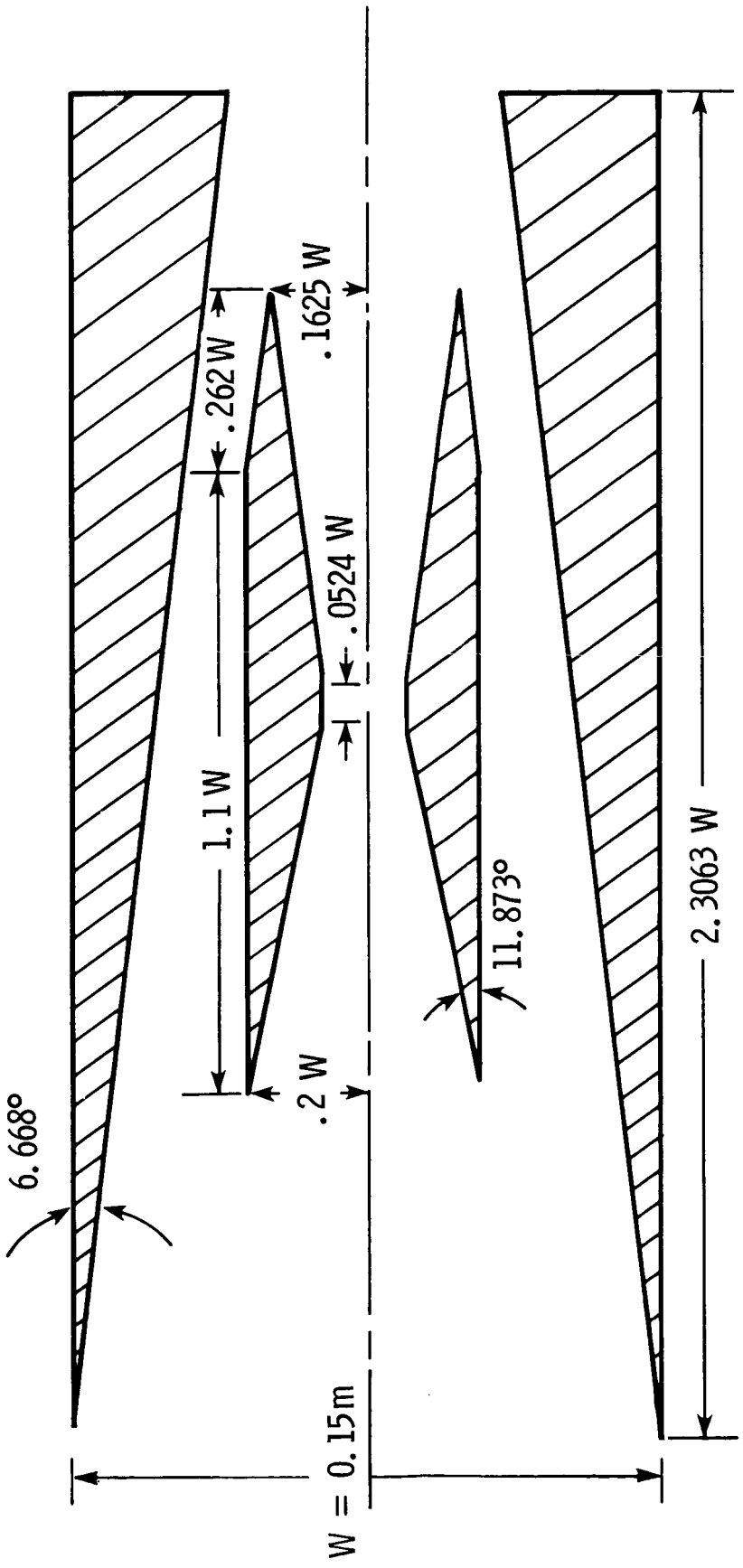

Figure 12.- Geometry of a two-strut inlet in a plane normal to sidewall leading-edge sweep.

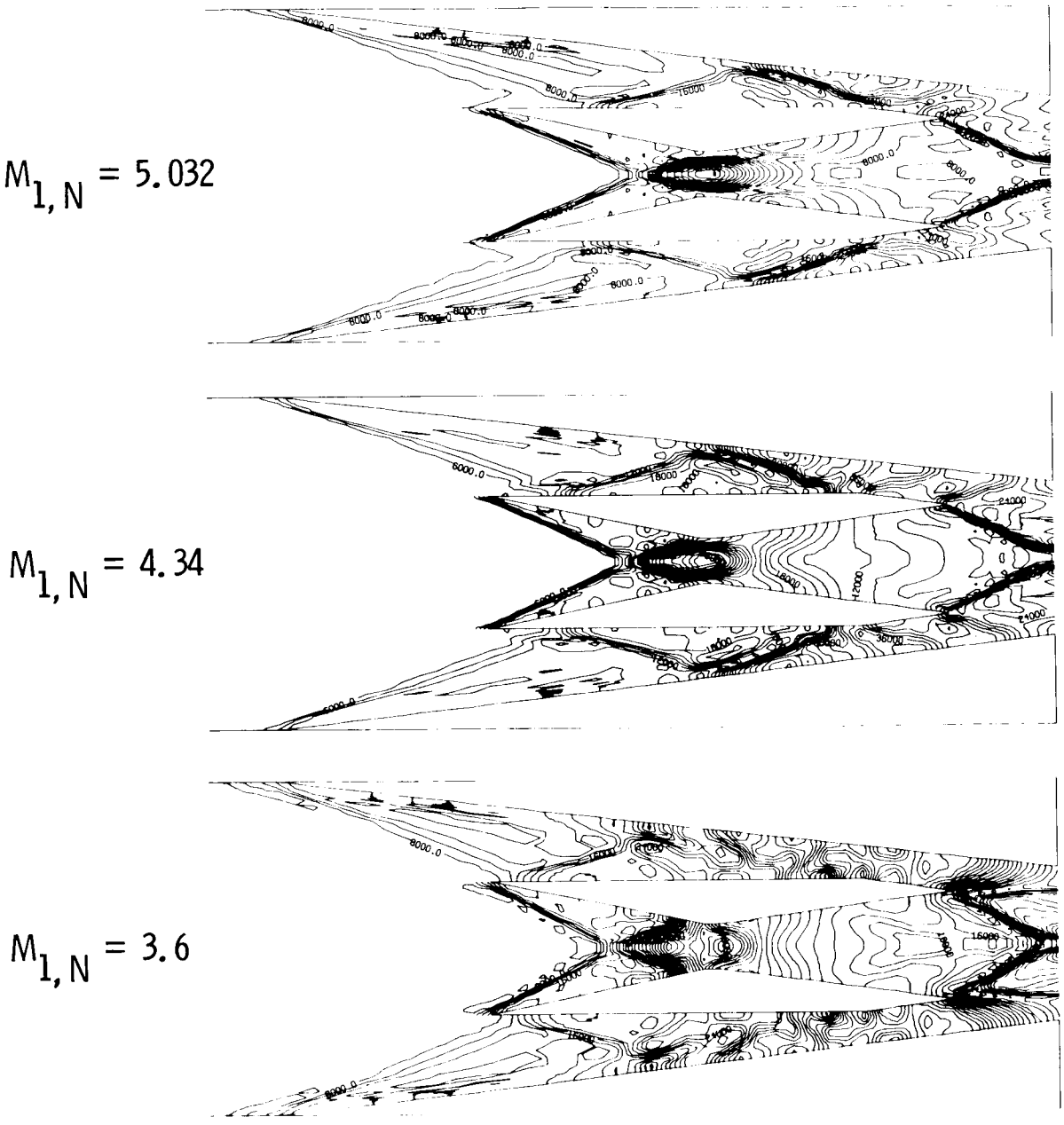

Figure 13.- Pressure contours for laminar flow at three Mach numbers.

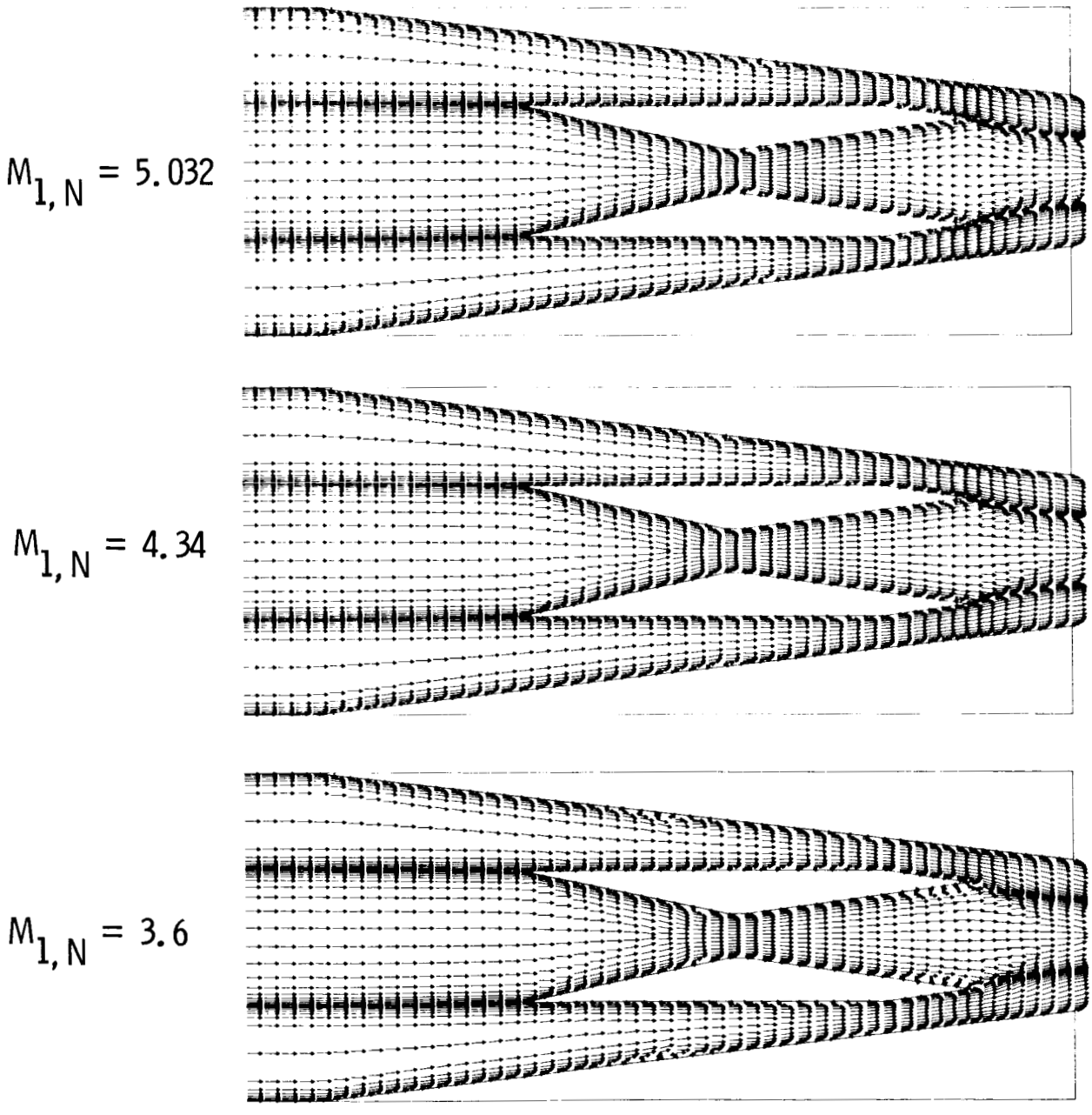

Figure 14.- Velocity-vector fields for laminar flow at three Mach numbers.

1. Report No.	2. Government Accession No.	3. Recipient's Catalog No.
NASA TP-1940		

4. Title and Subtitle	5. Report Date
NUMERICAL ANALYSIS OF THE SCRAMJET-INLET FLOW FIELD BY USING TWO-DIMENSIONAL NAVIER-STOKES EQUATIONS	December 1981
	6. Performing Organization Code: 505-32-93-01

7. Author(s)	8. Performing Organization Report No.
Ajay Kumar	L-14776
	10. Work Unit No.

9. Performing Organization Name and Address	11. Contract or Grant No.
NASA Langley Research Center Hampton, VA 23665	
	13. Type of Report and Period Covered: Technical Paper

12. Sponsoring Agency Name and Address	14. Sponsoring Agency Code
National Aeronautics and Space Administration Washington, DC 20546	

15. Supplementary Notes

16. Abstract

A computer code has been developed to solve the full two-dimensional Navier-Stokes equations in a supersonic combustion ramjet (scramjet) inlet. In order to be able to consider a general inlet geometry with embedded bodies, a numerical coordinate transformation is used which generates a set of boundary-fitted curvilinear coordinates. The explicit finite-difference algorithm of MacCormack is used to solve the governing equations. An algebraic, two-layer eddy-viscosity model is used for the turbulent flow. The code can analyze both inviscid and viscous flows with no strut, one strut, or multiple struts in the flow field. The application of the two-dimensional analysis in the preliminary parametric design studies of a scramjet inlet is discussed briefly. Detailed results are presented for one model problem and for several actual scramjet-inlet configurations.

17. Key Words (Suggested by Author(s))	18. Distribution Statement
Scramjet inlet Navier-Stokes equations Hypersonic propulsion	Unclassified - Unlimited Subject Category 07

19. Security Classif. (of this report)	20. Security Classif. (of this page)	21. No. of Pages	22. Price
Unclassified	Unclassified	28	A03

For sale by the National Technical Information Service, Springfield, Virginia 22161

NASA-Langley, 1981